Supplemental information

Tetravalent SARS-CoV-2 Neutralizing Antibodies Show Enhanced Potency and Resistance to Escape Mutations

Shane Miersch, Zhijie Li, Reza Saberianfar, Mart Ustav, James Brett Case, Levi Blazer, Chao Chen, Wei Ye, Alevtina Pavlenco, Maryna Gorelik, Julia Garcia Perez, Suryasree Subramania, Serena Singh, Lynda Ploder, Safder Ganaie, Rita E. Chen, Daisy W. Leung, Pier Paolo Pandolfi, Giuseppe Novelli, Giulia Matusali, Francesca Colavita, Maria R. Capobianchi, Suresh Jain, J.B. Gupta, Gaya K. Amarasinghe, Michael S. Diamond, James Rini, Sachdev S. Sidhu

Table S1. X-ray Data collection and refinement statistics

Structure	RBD-Fab 15033	RBD-Fab 15033-7
PDB	**7KLG**	**7KLH**
Data collection		
Wavelength (Å)	1.522	1.522
Resolution range (Å)	47.99 - 3.2 (3.314 - 3.2)	49.32 - 3.0 (3.107 - 3.0)
Space group	P 63 2 2	P 63 2 2
Unit cell	197.1 197.1 211.51 90 90 120	197.27 197.27 211.09 90 90 120
Total reflections		637956 (62437)
Unique reflections	40507 (3971)	48942 (4825)
Multiplicity	12.9 (13.3)	13.0 (12.9)
Completeness (%)	99.42 (99.90)	99.60 (99.83)
Mean I/sigma(I)	8.78 (1.11)	13.15 (0.93)
Wilson B-factor	92.69	95.02
R-merge	0.2504 (2.626)	0.1579 (2.764)
R-meas	0.2606 (2.726)	0.1644 (2.88)
R-pim	0.07087 (0.7218)	0.04501 (0.7978)
CC1/2	0.998 (0.585)	0.999 (0.42)
CC*	0.999 (0.859)	1 (0.769)
Refinement Statistics		
Reflections used in refinement	40303 (3969)	48784 (4821)
Reflections used for R-free	2018 (198)	2440 (241)
R-work	0.2754 (0.4048)	0.2599 (0.4154)
R-free	0.2960 (0.4220)	0.2881 (0.4343)
CC(work)	0.925 (0.647)	0.947 (0.544)
CC(free)	0.915 (0.583)	0.923 (0.478)
Number of non-hydrogen atoms	9717	9705
macromolecules	9689	9677
ligands	28	28
Protein residues	1270	1270
RMS bond length (Å)	0.004	0.003
RMS bond angle (°)	0.72	0.59
Ramachandran favored (%)	95.15	96.34
Ramachandran allowed (%)	4.69	3.58
Ramachandran outliers (%)	0.16	0.08
Rotamer outliers (%)	0	0
Clashscore	4.25	2.83
Average B-factor	96.78	103.02
macromolecules	96.75	102.97
ligands	108.19	120.94

Table S2. Cryo-EM data collection and image processing

Structure	spike, 2x Fab 15033-7 2-"up"-1-"down"	spike, 3x Fab 15033-7 3-"up", C3-symmetric	spike, 3x Fab 15033-7 3-"up", asymmetric	spike, 3x Fab 15033-7 2-"up", 1-"down"
EMDB ID	**EMD-22925**	**EMD-22926**	**EMD-23064**	**EMD-23065**
PDB ID	**7KMK**	**7KML**	**7KXJ**	**7KXK**
Data collection				
Electron microscope	Titan Krios G3			
Camera	Falcon 4EC			
Voltage	300 kV			
Nominal magnification	75000x			
Calibrated physical pixel size (Å)	1.03			
Total exposure (e/Å2)	38			
Number of fractions	30			
Movies collected	6431			
Image Processing and map refinement				
Motion correction software	cryoSPARC v2			
CTF estimation software	Gctf			
Particle selection software	cryoSPARC v2			
Classification and refinement software	cryoSPARC v2			
symmetry	C1	C3	C1	C1
Global resolution (Å)	4.2	3.8	6.4	5.0
Particles used in final reconstruction	88121	95627	19743	32257
Structural refinement				
Modeling software	Coot, Rosetta, Phenix			
RMS bond length (Å)	0.019	0.018	0.020	0.018
RMS bond angle (°)	1.84	1.88	1.91	1.84
MolProbity score	0.77	0.68	0.75	0.77
Clash score	0.79	0.53	0.79	0.88
Ramachandran favored	97.95%	98.14%	98.38%	98.03%
Ramachandran outliers	0.08%	0.00%	0.07%	0.07%
Rotamer outliers	0.17%	0.39%	0.18%	0.42%
Cbeta outliers	0.03%	0.00%	0.05%	0.07%
Average B factor (protein)	352	259	649	505
Average B factor (glycan)	381	248	660	412

Figure S1

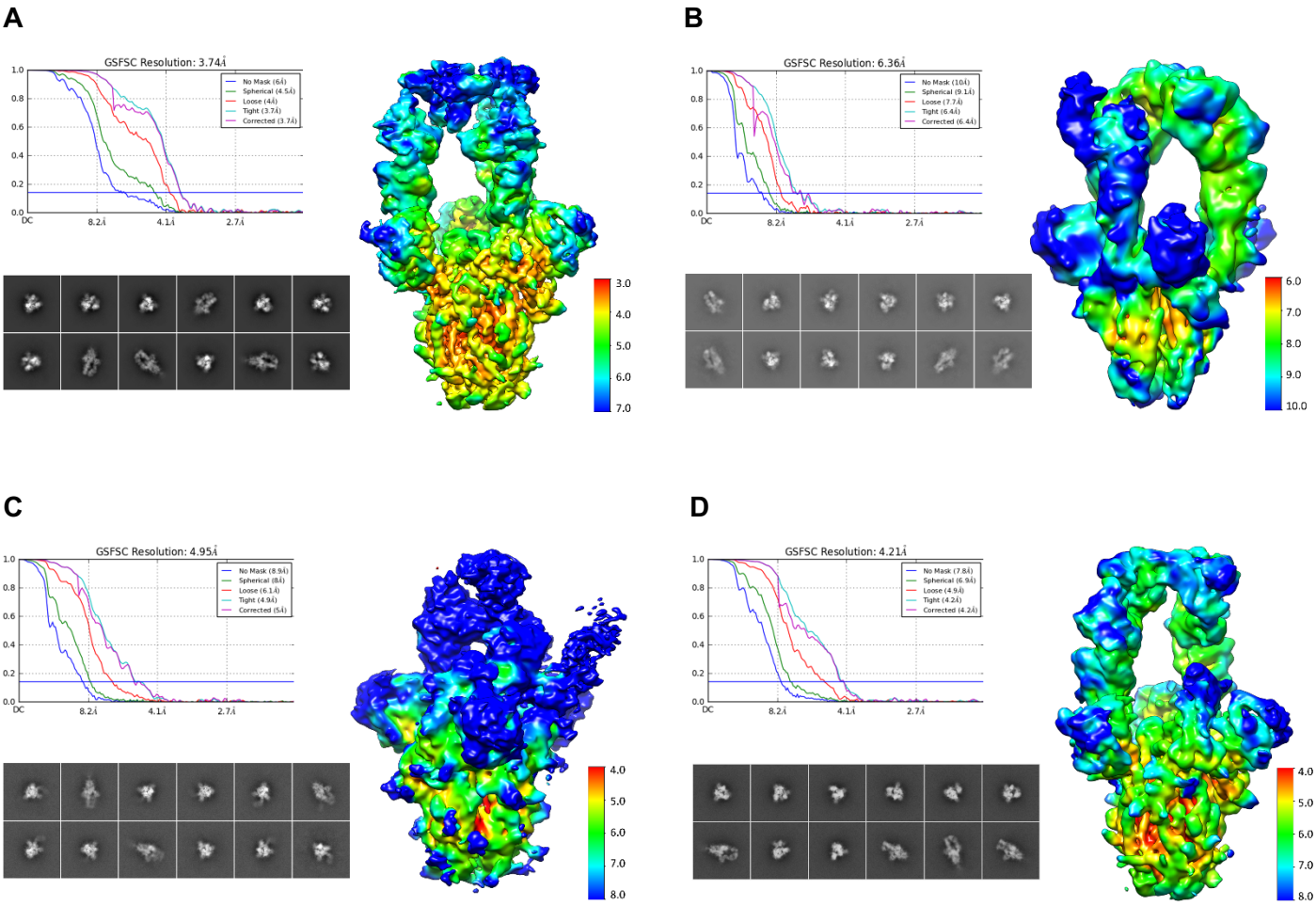

Figure S1. 2D class averages and resolution plots of the four 15033-7 Fab-S-protein cryo-EM structures The GSFSC curve, selected 2D class averages and the local resolution map are shown for each of the four structures: **A)** the 3-Fab-bound, 3-"up", C3 symmetric structure; **B)** the 3-Fab-bound, 3-"up", asymmetric structure; **C)** the 3-Fab-bound, 2-"up"-1-"down" structure; **D)** the 2-Fab-bound, 2-"up" structure.

Figure S2. Cryo-EM maps showing only Fabs and RBDs in the density (on next page) **A-D)** The 15033-7 Fabs (colored ribbons) are shown in the cryo-EM maps for each of the four structures: **A)** the 3-Fab-bound, 3-"up", C3 symmetric structure; **B)** the 3-Fab-bound, 3-"up", asymmetric structure; **C)** the 3-Fab-bound, 2-"up"-1-"down" structure; "A", "B" and "C" label the three Fab-RBD units where "C" is in the "down" conformation, "A" stacks over "C" and "B" is the Fab-RBD unit pushed away from the 3-fold rotation axis; **D)** the 2-Fab-bound, 2-"up" structure; **E)** A top view of the "B" Fab-RBD unit (Fab, orange; RBD, green) shown in **C)**. **F)** Comparison of the 15033-7 Fab-RBD unit found in the C3 symmetric cryo-EM structure (Fab, blue; RBD, green) with that found in the crystal structure (Fab and RBD, gray). A change in the Fab elbow angle is observed. **G)** The Fab-RBD unit in the C3 symmetric cryo-EM map, showing two views. **H)** Local-refinement map of the 15033-7 Fab-RBD unit, showing two views. In **G)** and **H)** the Fab heavy chain, Fab light chain and the RBD are colored blue, magenta and green, respectively.

Figure S2

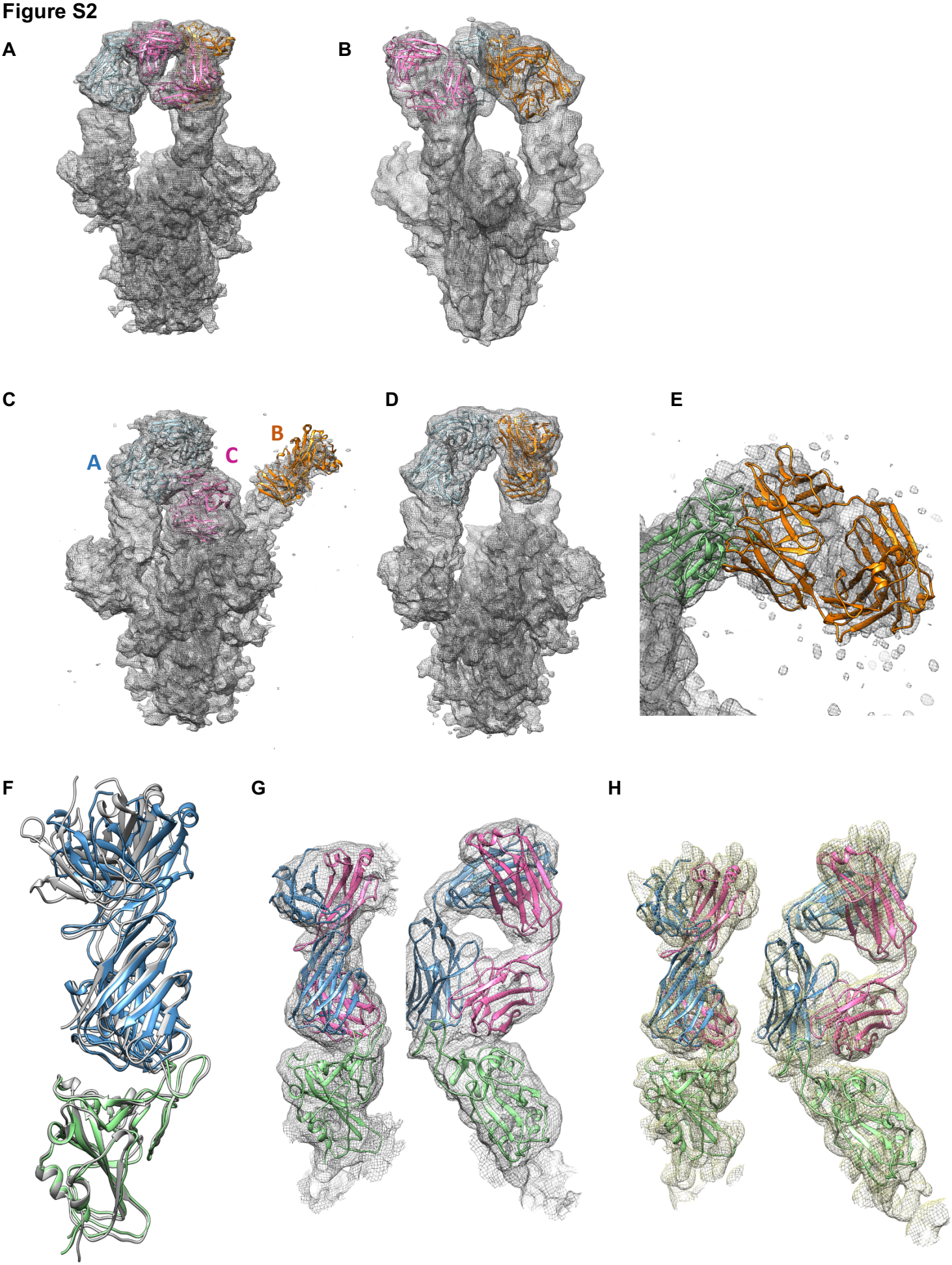

Figure S3

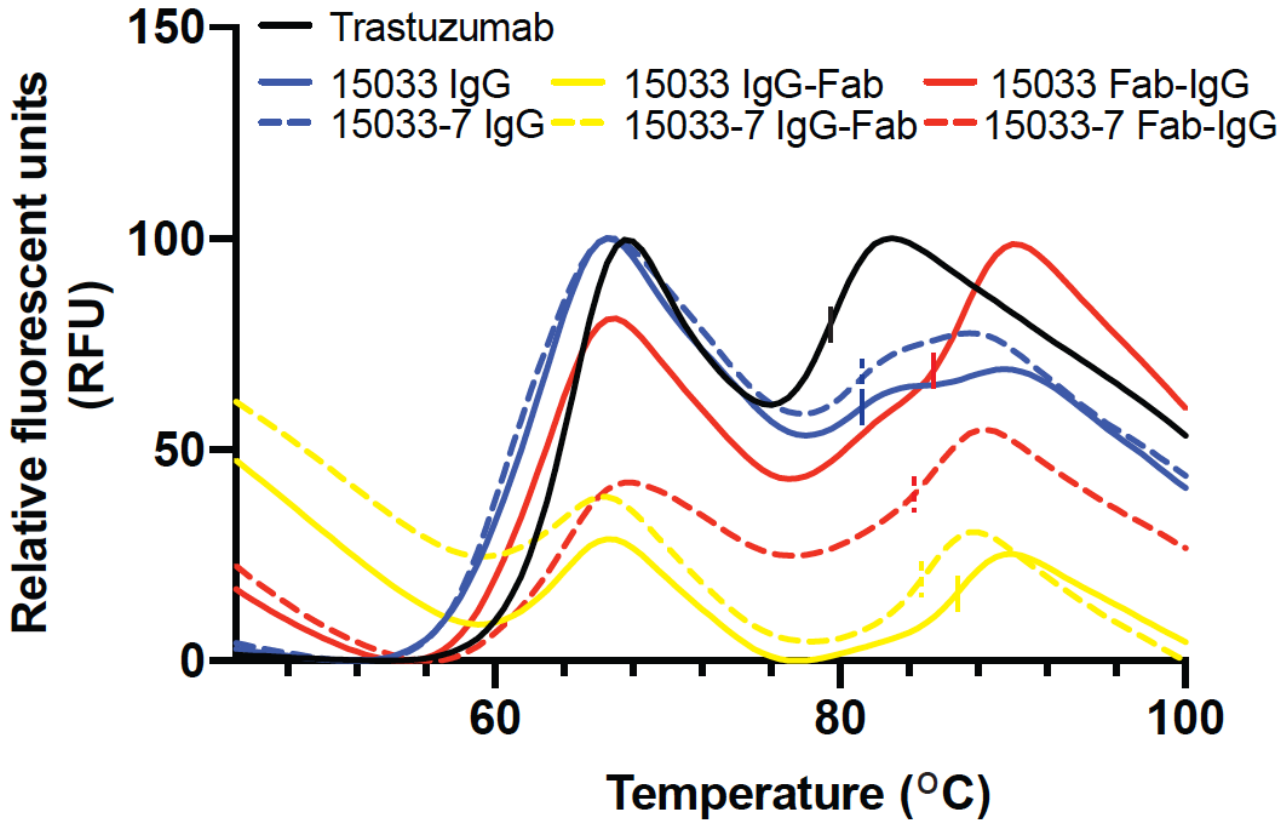

Figure S3. Thermostability of 15033 IgG and tetravalent antibodies and matured variants Thermal melt curves obtained by monitoring the fluorescence of Sypro orange in the presence of 1 μM antibody from 44 - 100 °C and the relative fluorescence intensity baseline shifted to zero. Vertical bars mark the point of inflection in each curve indicating the T_M2.

.

Figure S4

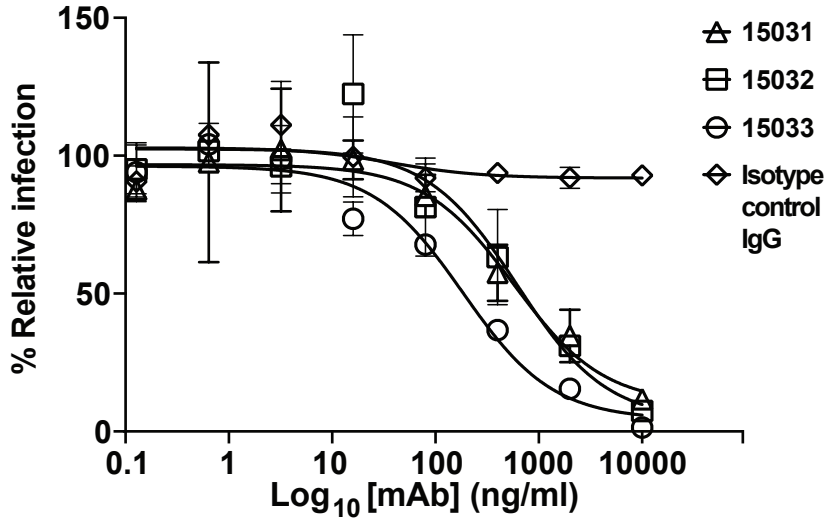

Figure S4. Antibody-mediated neutralization of clinically isolated SARS CoV2 virus Infection of VeroE6 cells by a clinically-isolated SARS CoV2 virus (strain 2019 n-CoV/USA_WA1/2020) was measured over a range [IgG] versus an IgG isotype control antibody using a focal reduction neutralization assay. Relative infection determined from the number of detectable foci was plotted versus log-transformed [IgG] and plots fit to determine IC_{50} values.

Figure S5

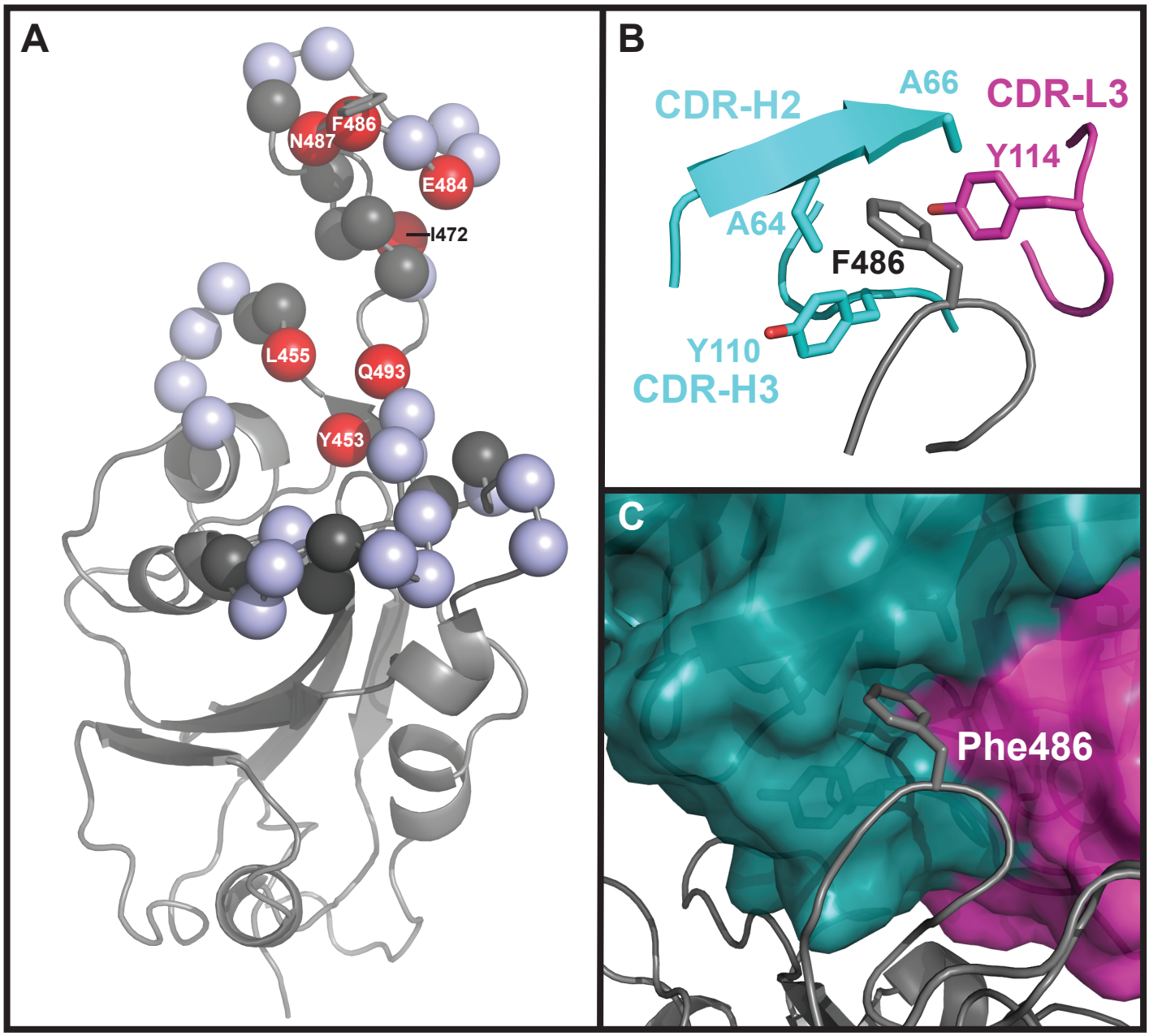

Figure S5. Vulnerabilities of antibody-mediated neutralization to potential escape mutants. (A) RBD residues individually mutated to alanine are indicated by spheres and labeled with the residue number. Those variants that exhibited reduced infection >75% relative to the wt are shown in dark grey and were not included in the analysis; those that exhibited at least 25% infectivity but could be neutralized >95% by 50 nM IgG 15033 are shown in light grey and those that retained infectivity but exhibited <95% neutralization of infection by 50 nM IgG 15033 are shown in red. **(B)** Residue Phe486 and Fab CDR residues within 4 Å of it are shown from the crystal structure of the complex of Fab 15033-7 and the SARS CoV-2 RBD. **(C)** Surface view of Fab 15033-7 in complex with the RBD reveals that residues in **(B)** form a hydrophobic pocket between the heavy and light chain, into which Phe486 inserts.

Figure S6

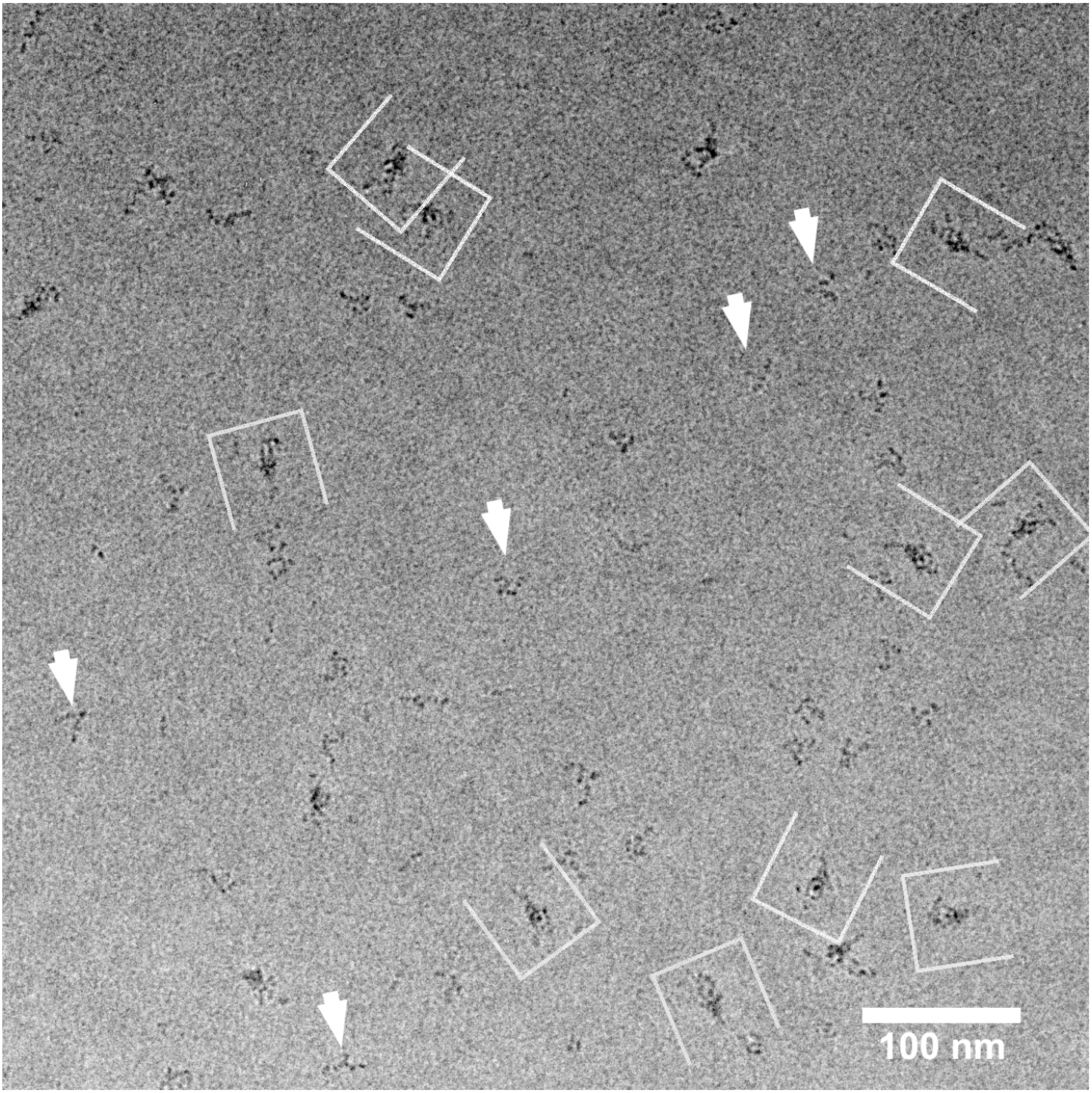

Figure S6. A negative stain micrograph of the Fab-IgG-S-protein complex The Fab-IgG-S-protein complexes are indicated by open brackets. Unbound Fab-IgG molecules are indicated by white arrowheads. The micrograph is contrast-inverted to help visualization.

Figure S7

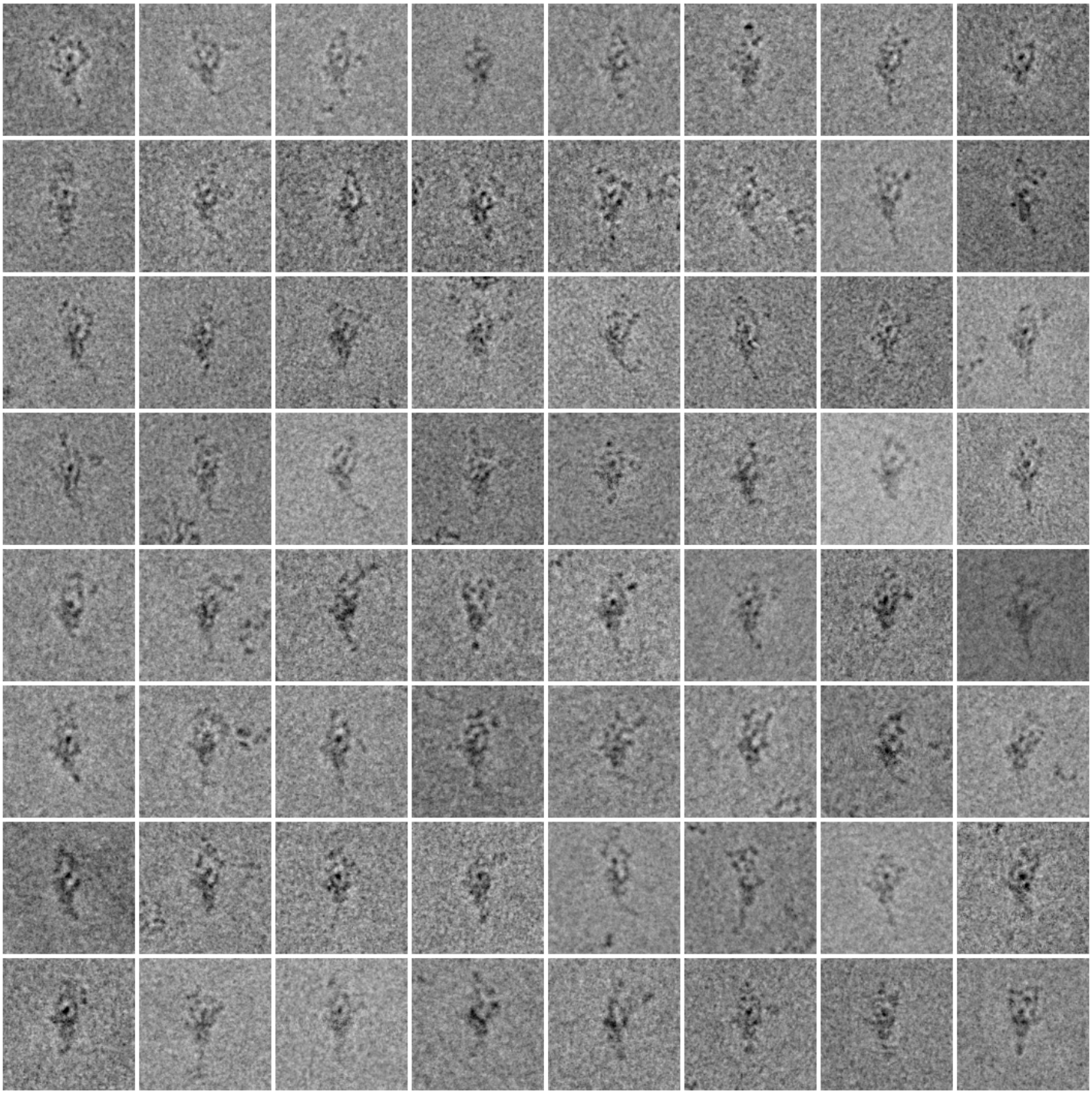

Figure S7. Negative stain EM particle images of the Fab-IgG-S-protein complexes Each panel contains a Fab-IgG-S-protein complex observed in negative stain EM micrographs. Each particle is aligned so that the spike portion is upright. The images are contrast-inverted to help visualization.